Saudi Dental Journal (2021) 33, 248–255

King Saud University

Saudi Dental Journal

www.ksu.edu.sa
www.sciencedirect.com

ORIGINAL ARTICLE

Evaluation of the regenerative potential of decellularized skeletal muscle seeded with mesenchymal stromal cells in critical-sized bone defect of rat models

Lujain hakeem [a,*], **Mohammed Al-Kindi** [a], **Nihal AlMuraikhi** [b], **Sarah BinHamdan** [c], **Ahmad Al-Zahrani** [a]

[a] *Department of Oral and Maxillofacial Surgery, College of Dentistry, King Saud University, Riyadh, Saudi Arabia*
[b] *Stem Cell Unit, Department of Anatomy, College of Medicine, King Saud University, Riyadh, Saudi Arabia*
[c] *College of Medicine, Al-Faisal University, Riyadh, Saudi Arabia*

Received 10 February 2021; revised 8 March 2021; accepted 9 March 2021
Available online 22 March 2021

KEYWORDS

Bone bioengineering;
Decellularized skeletal muscle graft;
Critical bone defect

Abstract *Background:* The morbidities and complications reported in the reconstruction of large bony defects have inspired progression in the field of bioengineering, with a recent breakthrough for the use of decellularized skeletal muscle grafts (DSMG).

Aim: To assess the osteogenic potentials of seeded DSMG *in vitro* and to investigate bone regeneration in critical size defect *in vivo*.

Materials and Methods: Assessment of cell viability and characterization was carried out on seeded DSMG for different intervals *in vitro*. For *in vivo* experiments, histological analysis was performed for rat cranial defects for the following groups: (A) non-treated DSMG and (B) seeded DSMG after a period of 8 weeks.

Results: The *in vitro* experiment demonstrated the lack of cytotoxicity and inert properties of seeded DSMG; these facilitated the osteogenic differentiation and significant gene expressions, particularly of *COL1A1*, *RUNX2*, and *OPN* (1.9174 ± 0.11673, 1.1806 ± 0.02383, and 1.1802 ± 0.00775, respectively). In the *in vivo* experiment, superior results were detected in the seeded DSMG group which showed highly vascularized and cellular dense connective tissue with deposited bone matrix and multiple scattered islets of newly formed bone.

* Corresponding author.
E-mail addresses: lhakeem@ksu.edu.sa (L. hakeem), mAlKindi@ksu.edu.sa (M. Al-Kindi), nalmuraikhi@ksu.edu.sa (N. AlMuraikhi), azahran@KSU.EDU.SA (A. Al-Zahrani).

Peer review under responsibility of King Saud University.

Production and hosting by Elsevier

https://doi.org/10.1016/j.sdentj.2021.03.006

Conclusion: Our results demonstrated the promising aspects of DSMG; however, there is a lack of studies to support further implications.

1. Introduction

Inadequate vascularity, nutritional background, and tissue sustainability have always been the main difficulties in the reconstruction of critical bone defects in the head and neck region (Pogrel et al., 1997; Schliephake, 2009). Therefore, to address the problem of insufficient angiogenesis with engineered grafts, studies have suggested the use of skeletal muscle as a bioreactor to optimize bone regeneration and vasculature (Heliotis et al., 2006 Ayoub et al., 2007; Badylak & Gilbert, 2008; Kokemueller et al., 2010; Liu et al., 2011; Oryan et al., 2014; Alfotawi et al., 2017, 2016). However, these promising results are also accompanied by some limitations, including donor site morbidity and inadequate graft availability. A breakthrough study by Aulino et al. (2015) demonstrated the use of decellularized skeletal muscle grafts (DSMG) at the interface between muscle and bone in an animal model. Their study showed matrix mineralization at a site nearest to the bone, suggestive of the osteogenic potential of DSMG. This breakthrough result has also emphasized the advantages of DSMG in preserving the three dimensions of the vascular network and its reduced immunogenicity properties (Criswell et al., 2013; Porzionato et al., 2015). These interesting facts support the possible use of DSMG as an allograft material in a clinical setting to reduce donor site morbidity. Nevertheless, to our knowledge, there is limited evidence supporting the use of DSMG in restoring craniofacial region defects. The scope of this paper was to study the bone regeneration ability of DSMG infused with mesenchymal stromal cells (MSC) to reconstruct critical-size bone defects.

2. Materials and methods

2.1. Ethical guidelines

Approval from the Ethical Committee was obtained from the Institutional Animal Care and Use Committee of the King Saud University College of Medicine Research Center and College of Dentistry Research Center. The study was conducted using the facilities and support of the Stem Cell Unit, the Experimental Surgery and Animal Laboratory at King Saud University in Riyadh, Saudi Arabia.

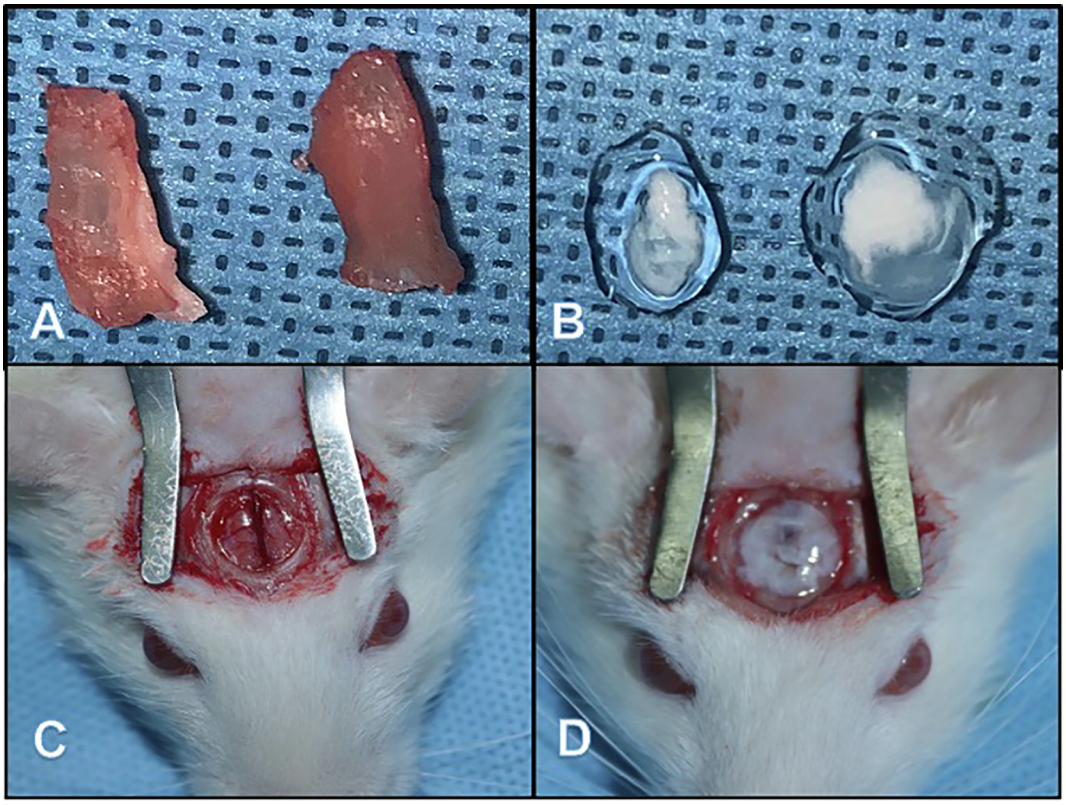

Fig. 1 (A) Sliced Fresh bovine source skeletal muscle tissue (Pre- decellularization). (B) Sliced prepared scaffold (Decellularized muscle graft). (C) 8 mm calvarial defect created by trephine bur. (D) DSMG placed in the defect.

2.2. In vitro experiment

2.2.1. Scaffold decellularization preparation

Fresh, bovine-sourced skeletal muscle tissues measuring 8 mm × 2 mm were sliced and placed in a 24-well plate. Porzionato et al.'s (2015) protocol was followed for scaffold decellularization (Fig. 1A-B).

2.2.2. Cell line, culture, and seeding

The human telomerase reverse transcriptase (hMSC-TERT) cell line was used in this experiment as a model for human bone marrow stem cells (hBMSCs) (Simonsen et al., 2002; Abdallah et al., 2005). Herein, 1×10^6 cells were cultured in Dulbecco's modified Eagle medium (DMEM) (Gibco Invitrogen), which contains 4500-mg/L D-glucose, 4-mML-glutamine, and 110-mg/L 10% sodium pyruvate; the medium was supplemented with 10% fetal bovine serum (FBS), 1% penicillin–streptomycin, and 1% nonessential amino acids (Thermo Fisher Scientific, USA). Cells were incubated in a 5% CO_2 incubator at 37 °C, and the medium was changed every 2–3 days. After reaching a confluence of 80%–90%, concentrations of 6×10^4 and 1×10^6 were used for *in vitro* and *in vivo* experiments, respectively. In addition, different seeding techniques were used according to the study group (Merritt et al., 2010; Villalona et al., 2010).

2.2.3. Cell characterization and osteogenic differentiation

Cultured cells were treated with osteoblast induction medium containing 10% FBS, 1% penicillin–streptomycin, 50-µg/mL L-ascorbic acid (Wako Chemicals GmbH ,Germany), 10-nM b-glycerophosphate (Sigma-Aldrich, Germany), 10-nM calcitriol (Sigma-Aldrich), and 10-nM dexamethasone (Sigma-Aldrich, Germany). Treatment was maintained for 14 and 21 days before proceeding with any analysis.

2.2.4. Morphological assessment

2.2.4.1. 4′,6-diamidino-2-phenylindole (DAPI) for assessment of DSM. Immediately after the decellularization of the skeletal muscle, DSMG samples were stained with DAPI stain (Thermo Fisher Scientific,USA), following the manufacturer's sample preparation guidelines. They were then examined under a fluorescent microscope (Nikon®, Eclipse Ti2 inverted microscope) with an excitation filter of 355–425 nm to assess the cellularity of the scaffolds.

2.2.4.2. Histological examination of the DSMG. Histological analysis was carried out immediately after decellularization to confirm complete decellularization of the prepared DSMG. This DSMG was then fixed in ice-cold paraformaldehyde and dehydrated in graded ethanol. Next, 5-µm embedded paraffin sections were stained with hematoxylin and eosin (H&E) and evaluated under light microscopy (Zeiss®, Axio Observer A1 inverted microscope).

2.2.4.3. Scanning electron microscopy (SEM). JSM-6360 LV SEM was used for the assessment of the morphological microstructure of DSMG and cell attachment after 48 h of seeding. In brief, the samples were fixed in 2.5% glutaraldehyde and then fixated with 1% osmium tetroxide following the manufacturer's instructions. Thereafter, samples were dehydrated with graded ethyl alcohol and dried by using CO_2. Finally, the samples were coated with a gold spatter coater.

2.2.5. Viability and proliferation assays

Cell viability was determined by AlamarBlue® assay (Thermo Fisher Scientific) at three different time intervals (3, 5, and 7 days). Two experimental groups were used for the analysis: (1) a control (hMSC-TERT cell seeded in empty wells) and (2) a hMSC-TERT cell line seeded into DSMG. At each time point, the wells were cultured with AlamarBlue® substrate and incubated in the dark at 37 °C for 4 h. The analysis was completed using a BioTek Synergy II microplate reader (BioTek Inc., Winooski, VT, USA), with Gen5 data analysis software (BioTek®, Winooski, VT, USA) and fluorescent mode (Ex 530 nm/Em 590 nm).

2.2.6. Differentiation assay

2.2.6.1. Quantitative reverse transcription-polymerase chain reaction (qRT-PCR). Cells were cultured in osteoblast induction medium based on the group assembly: (1) induced hMSC-TERT and (2) induced hMSC-TERT seeded into DSMG. Total RNA was isolated after 14 and 21 days following the manufacturer's instructions for the RNAase extraction kit (Analytik Jena AG). The concentrations of total RNA were measured using NanoDrop 2000 spectrophotometer (Thermo Fisher Scientific, USA), Complementary DNA (cDNA) synthetization using the Thermo Fisher Scientific High-Capacity cDNA transcription kit and ProFlex PCR system followed. Gene expression levels were determined using real-time PCR (Thermo Fisher Scientific—VIA 7 system) with the use of a

Table 1 Characteristics of the primers used in the study.

Gene	Primer sequence (5′-3′ (forward/reverse))
Runt-related transcription factor 2 (RUNX2)	Forward: CACCATGTCAGCAAAACTTCTT Reverse: ACCTTTGCTGGACTCTGCAC
Alkaline phosphatase (ALP)	Forward: GACGGACCCTCGCCAGTGCT Reverse: AATCGACGTGGGTGGGAGGGG
Osteocalcin (OSC)	Forward: GGCAGCGAGGTAGTGAAGAG Reverse: CTCACACACCTCCCTCCTG
Osteopontin (OPN)	Forward: CAGTTCAGAAGAGGAGG Reverse: TCAGCCTCAGAGTCTTCATC
Collagen Type I Alpha 1 (COL1A1)	Forward: GAGTGCTGTCCCGTCTGC Reverse: TTTCTTGGTCGGTGGGTG
Glyceraldehyde 3-phosphate dehydrogenase (GAPDH)	Forward:CTGGTAAAGTGGATATTGTTGCCAT Reverse: TGGAATCATATTGGAACATGT

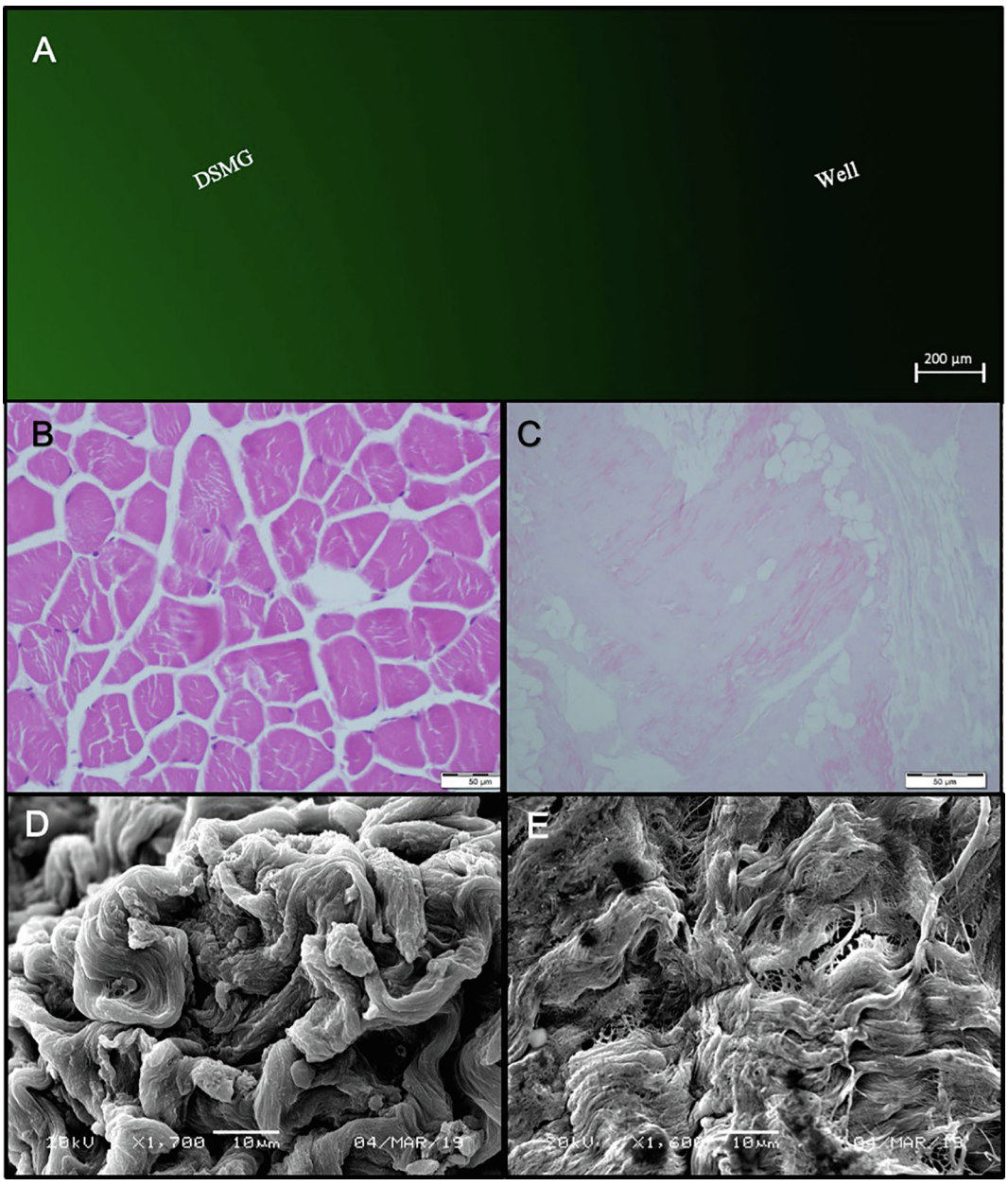

Fig. 2 (A) Stained DSMG examined under the fluorescent microscope. Scale bar = 200 µm. (B) H & E of native muscle tissue, with the presence of cell nuclei. (C) Prepared scaffold (Decellularized muscle graft) with absence of cells, and preservation of extracellular matrix. Scale bar = 50 µm. (D) SEM of decellularized skeletal muscle graft, with preserved collagenic muscle fibers after treatment and absence of myocytes. (E) DSMG after 48 h of cell seeding with evident of cell attachment over DSMG.

quantitative reverse transcriptase-polymerase chain reaction (qRT-PCR) kit (Applied Biosystem, UK) to amplify the targeted osteogenesis-related genes (Table. 1). Normalization to the reference gene GAPDH, the qRT-PCR products were quantified using the previously described $2^{-\Delta\Delta Ct}$ method (Spicer et al., 2012).

2.3. In vivo experiment

2.3.1. Study design and model

The study was carried out as a case-control study of the proposed hypothesis with a comparison between two groups (Group A: non-treated DSMG; Group B: seeded DSMG) and aimed to evaluate bone regeneration in critical-size defects by the use of DSMG infused with rat MSC. Ten adult Sprague–Dawley rats comprised each group, as the sample size selected was based on a standard deviation of 0.7 and a maximum difference of 0.8 with a power of 0.85.

2.3.2. Culture and seeding of rat bone marrow stromal cells

Bone marrow was obtained from Sprague–Dawley rats, as previously described (Zhang & Chan, 2010). Then, cells were cultured and maintained in DMEM. Passage two was used after reaching a confluence of 80%–90% with a density of 1×10^6 in each DSMG. After seeding, the seeded grafts were incubated for 24 h before implementation.

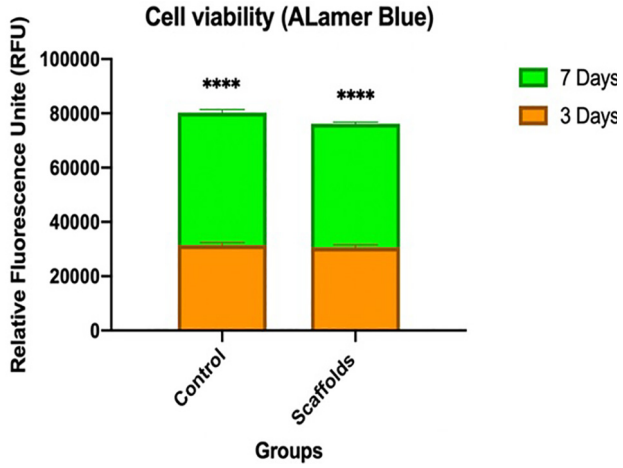

Fig. 3 Quantitative proliferation assay of hMSC-TERT cultured on well plate and DSMG scaffolds, showed increased cell proliferation rate with prolong culture time with statistical significant from day 3 to day 7 (Control: cell cultured in well plate, Scaffold: cell cultured in DSMG).

2.3.3. Surgery and sample collection

The protocol of the animal facility of King Khalid Hospital was used for sedation induction; the dose was calculated based on rat weight (0.2 mL/100 g). Spicer et al.'s (2013) protocol was used to create the calvarial defect. The defect was created by drilling with a slow-speed trephine bur with a depth of 1 mm and a diameter of 8 mm. Careful separation of the bone from the dura was completed without damaging the dura. The defect was washed copiously with sterile normal saline to remove any debris. We placed the treated bovine DSMG into the defect based on the experimental groups (Fig. 1C-D). Finally, the periosteum was scarified, and wound closure over the implanted scaffold was completed (Spicer et al., 2012). The pain was controlled by administering an NSAID analgesic (ketoprofen 10 mg/mL) by calculating the required dose based on animal weight (5 mg/kg once daily) (UBC Animal Care Guidelines, 2016) (https://animalcare.ubc.ca). Following the American Veterinary Medical Association guidelines for the euthanasia of animals (2020), the rats were euthanized eight weeks after the anesthetic agent overdose. The cranial defect sites were harvested and transferred into labeled containers with 10% formalin for further analysis.

2.3.4. In vivo assessment

2.3.4.1. Decalcification slides for histological assessment. Specimens were decalcified using a formic acid solution (0.4 M formic acid and 0.5 M sodium formate). Then, each specimen was divided into upper, middle, and lower sections. Paraffin-embedded tissue blocks were sectioned at 5 μm with an orientation paralleling the sagittal suture. For qualitative analysis, paraffin-embedded implants were stained with H&E stains. The slides were examined with the Aperio ImageScope - Pathology Slide Viewing software.

2.4. Statistical analysis

Statistical analysis and graphing were performed using GraphPad Prism 6 software. Results were presented as mean ± SEM. Unpaired *t* test was used to determine statistical significance as P values < 0.05 were considered statistically significant.

3. Results

*3.1. **In vitro** assessment*

3.1.1. Morphological assessment of DSMG

The samples of DSMG revealed that the uptake of DAPI stain by the molecular component was lacking, thus indicating the absence of cellular nuclei (Fig. 2A). Furthermore, H&E staining revealed a clear difference between the native bovine skeletal muscle and DSMG. As typical features of native skeletal muscle, we observed myofibrillar elements encased in endomysium and surrounded by perimysium along with multiple peripherally located nuclei. In contrast, DSMG showed the absence of myofibrillar elements and cell nuclei as well as pre-

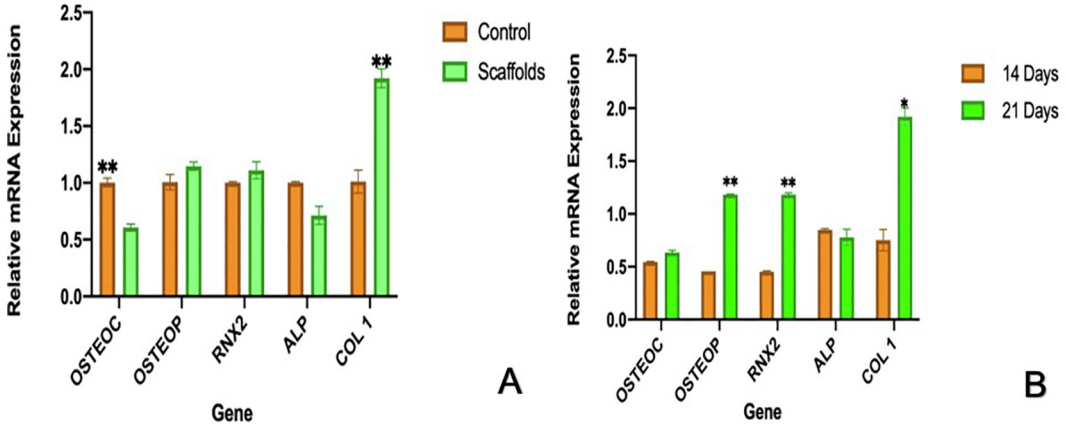

Fig. 4 (A) Osteogenic gene expression analysis of hMSC-TERT cells cultured in well plates, and on DSMG scaffolds. graph shows general gene expression with significant in expression of OSC in control group, and *COL1A1* ($p < 0.05$) in DSMG group ($p < 0.05$). (B) Osteogenic gene expression analysis of hMSC-TERT cells grown on DSMG scaffold for two intervals. Diagram shows significant upregulation of *COL1A1* , *RUNX2,* and *OPN* ($p < 0.05$) in 21 days compare to 14 days. Exception to that, slight down regulation was observed in ALP with not statistically significant.

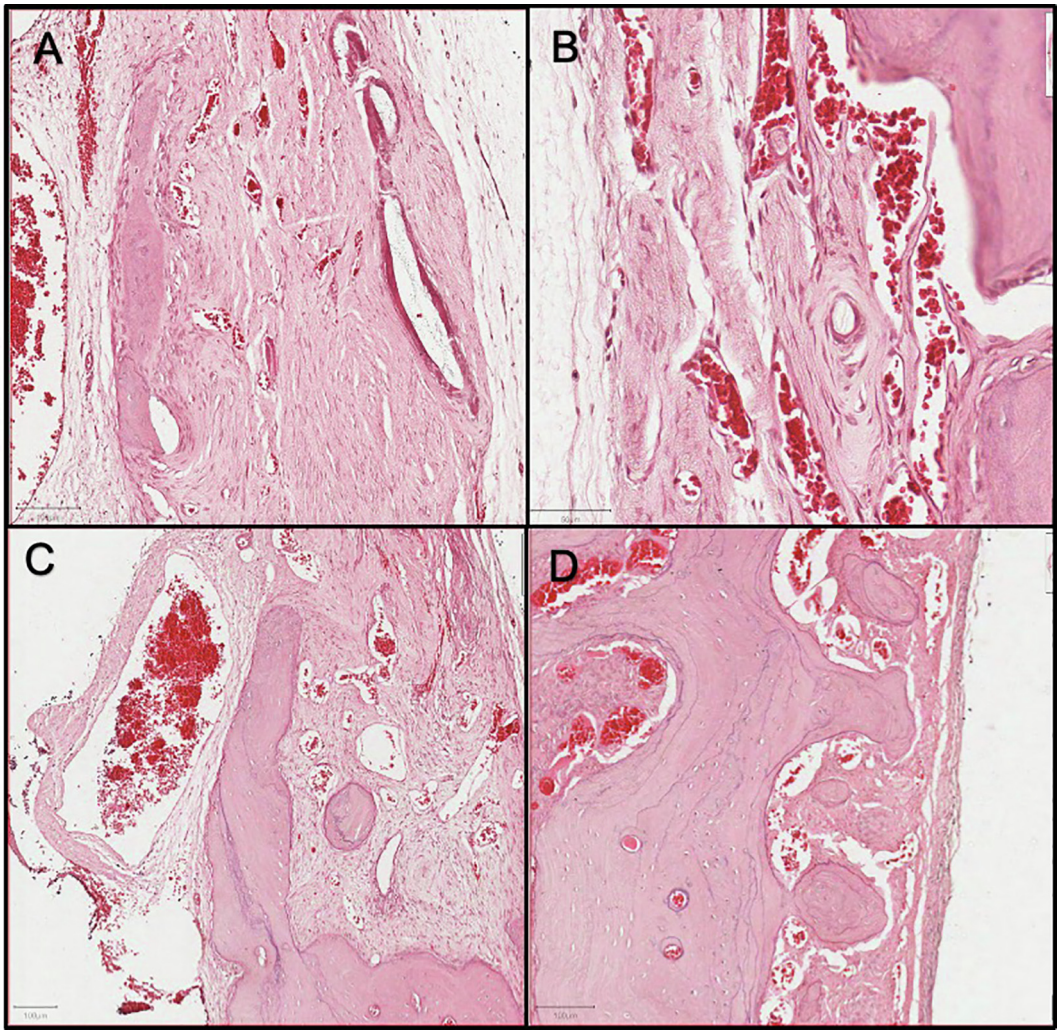

Fig. 5 Decalcified histological sections stained with H & E. (A-B) Group A (untreated DSMG) showed connective tissue that is vascularized and cellular with a cell population of osteoblasts, pre-osteoblasts, and fibroblast along the defect. Small island of mature bone can be seen at the center of the defect. (C-D) group B (treated DSMG) showed scattered deposited bone matrix. Multiple mature bone projection at the edges of the defect and the center with obvious bone remodeling.

served extracellular matrix architecture (Fig. 2B-C). SEM assessment of the grafts revealed tightly packed thin myofibrils in a mesh-like pattern with a uniform diameter. The observed microstructure showed a wavy and parallel banding of collagen fibers, with the absence of visible muscle cells (Fig. 2D).

3.1.2. Cell function

Herein, SEM of seeded DSMG revealed cell attachment over the extracellular matrix after 48 h with spared morphology and extended filopodia. Moreover, there was increased cell-to-cell contact and bridging with cellular infiltration through the collagen bundles of the scaffold (Fig. 2E). The metabolic activity of hMSC-TERT grown on a well plate and DSMG was evaluated using AlamarBlue®. Both groups exhibited similar fluorescent intensity with no statistically significant difference in the three intervals. However, a statistically significant difference was observed in both groups with prolonged culture duration (control group, 48779.67 ± 1121.03; scaffold group, 45637.33, ± 584.90) (Fig. 3).

3.1.3. Differentiation assay

Molecular analysis was performed after 14 and 21 days to evaluate induced hMSC-TERT cells cultured on well plates and DSMG. A significant expression was observed of *COL1A1* (1.001 ± 0.06658; $p < 0.05$) in the scaffold group compared to the control (Fig. 4A). Moreover, the scaffold group showed significant upregulation in *COL1A1*, followed by *RUNX2* and *OPN* (1.9174 ± 0.11673, 1.1806 ± 0.02383, and 1.1802 ± 0.00775, respectively) with a prolonged culture time (Fig. 4B).

3.2. In vivo assessment

3.2.1. Histological assessment

The H&E stained decalcified histological sections of the defect revealed that both defects were not completely regenerated with bone but were filled with dense connective tissue. Superior results were expressed in the experimental group (seeded DSMG), which showed thick connective tissue with high

deposits of bone matrix packed with osteoblasts (Fig. 5). The defect appears highly vascular compared to the control group and is filled with multiple scattered islets of newly formed bone along the defect (Fig. 5).

4. Discussion

The current findings illustrate the promising potential of seeded DSMG. The morphological assessment corresponded to the findings of Porzionato et al. (2015), wherein successful decellularization was obtained using trypsin-EDTA and Triton X-NH4OH. Their technique is simple and reliable for muscle decellularization while balancing the elimination of the cellular components and maintaining the extracellular matrix (Porzionato A et al., 2015). The biocompatibility of the prepared grafts is an essential factor for successful regeneration. Accordingly, our results confirmed the reduced antigenicity of DSMG, allowing for proper cell proliferation. Al-Fotawi et al. (2020) exhibited a comparable cell proliferation rate using similar scaffolds and decellularization protocols. However, our findings showed analogous results in both groups with a greater percentage of viability on Day 7 compared to Day 3, with an increase of up to 1.5-fold. This was in contradiction with Al-Fotawi et al.'s result, which demonstrated clear variance in cell proliferation rate between the experimental and control groups (Al-Fotawi et al., 2020). More importantly, this study proves the osteogenic potential after recellularization through early and late phases of osteogenic differentiation and maturation. The expression of *COL1A1* was the highest, with a 3.8-fold increase noted from Day 14 to Day 21 day in the experimental group (Fig. 4B). Moreover, high expression of *ALP* was noted on Day 14, which was downregulated by Day 21. An increase in the expression of *COL1A1* reportedly results in the down-regulation of ALP manifesting in bone cell maturation in osteogenic differentiation, which was comparable to our findings (Malaval et al., 1994). *Runx2* and *OPN* showed high expression following *COL1A1* in 21 days, reaching up to 3-fold (Fig. 4B). The upregulation of *RUNX2* is reportedly essential in the osteogenic maturation phase to maintain high expression of *COL1A1* and *OPN*, which is in agreement with our observation (Maruyama et al., 2007).

In vivo application of DSMG for its osteoconductive and bone regenerative capacity has been illustrated in limited studies. Aulino et al. (2015) demonstrated the multipotency of decellularized skeletal muscle in a rat model. Similarly, Alfotawi el al. (2020) evaluated the use of human bone marrow stem cells seeded into muscle extracellular matrix and mixed with silicon calcium phosphate cement in nude mice and showed enhanced bone formation. Our findings correspond with previous studies in that we were able to show enhanced bone regeneration within the defect in both groups, with a superior result noted in seeded DSMG. The majority of the muscle graft was replaced with rich vascularized and cellular connective tissue with immature osteoid clumps (Fig. 5). This is superior to reported studies of untreated similar defects that showed only a thin fibrous band with no visible signs of bone formation along the defect (Takagi and Urist, 1982; Patel et al., 2008). The current study also showed different stages of maturation within the defect, with areas of bone remodeling at the edges and multiple scattered islets of newly formed bone (Fig. 5). The reason for such encouraging findings is the ability of DSMG to facilitate intramembranous ossification by acting as a bioreactor for the injected cells. In addition, the increased capacity of revascularization, allows cell recruitment and wound healing. However, none of the experimental groups showed full regeneration of the defect, which could be attributed to the time factor, as assessment over a longer period could be associated with additional bone regeneration and maturation. In addition, it could be due to the limited use of bone factors that accelerate bone formation (Liu et al., 2015; Miao et al. 2017).

5. Conclusion

The simplicity in the preparation of DSMG along with its revascularization and osteoconductive potential, provide innovative tools in regenerative medicine to overcome the reconstructive challenges in the craniofacial region. However, further research is necessary to support further implications.

Declaration of Competing Interest

The authors declare that they have no known competing financial interests or personal relationships that could have appeared to influence the work reported in this paper.

References:

Abdallah, B., Haack-Sorensen, M., Burns, J., Elsnab, B., Jakob, F., Hokland, P., Kassem, M., 2005. Maintenance of differentiation potential of human bone marrow mesenchymal stem cells immortalized by human telomerase reverse transcriptase gene despite of extensive proliferation. Biochem. Biophys. Res. Commun. 326 (3), 527–538.

Alfotawi, R., Ayoub, A., Tanner, K., Dalby, M., Naudi, K., McMahon, J., 2016. A Novel Surgical Approach for the Reconstruction of Critical-Size Mandibular Defects Using Calcium Sulphate/Hydroxyapatite Cement, BMP-7 and Mesenchymal Stem Cells-Histological Assessment. J. Biomater. Tissue Eng. 6 (1), 1–11.

Al-Fotawi, R., Muthurangan, M., Siyal, A., Premnath, S., Al-Fayez, M., El-Ghannam, Ahmad, Mahmood, A., 2020. The use of muscle extracellular matrix (MEM) and SCPC bioceramic for bone augmentation. Biomed. Mater. 15, (2) 025005.

Alfotawi, R., Shwaf, B., Kawaja, N., 2017. The use of muscle as a bone bioreactor: an ex vivo experiment. Int. J. Oral Maxillofac. Surg. 46, 199–200.

Aulino, P., Costa, A., Chiaravalloti, E., Perniconi, B., Adamo, S., Coletti, D., Marrelli, M., Tatullo, M., Teodori, L., 2015. Muscle Extracellular Matrix Scaffold Is a Multipotent Environment. Int. J. Med. Sci. 12 (4), 336–340.

Ayoub, A., Challa, S., Abu-Serriah, M., McMahon, J., Moos, K., Creanor, S., Odell, E., 2007. Use of a composite pedicled muscle flap and rhBMP-7 for mandibular reconstruction. Int. J. Oral Maxillofac. Surg. 36 (12), 1183–1192.

Badylak, S., Gilbert, T., 008. Immune response to biologic scaffold materials. Semin. Immunol. 20 (2), 109–116.

Criswell, Corona, B., Wang, Z., Zhou, Y., Niu, G., Xu, Y., Christ, G., Soker, S, 2013. The role of endothelial cells in myofiber differentiation and the vascularization and innervation of bioengineered muscle tissue in vivo. Biomaterials 34, 140–149. https://doi.org/10.1016/j.biomaterials.2012.09.045.

Heliotis, M., Lavery, K., Ripamonti, U., Tsiridis, E., di Silvio, L., 2006. Transformation of a prefabricated hydroxyapatite/osteogenic protein-1 implant into a vascularised pedicled bone flap in the human chest. Int. J. Oral Maxillofac. Surg. 35 (3), 265–269.

Kokemueller, H., Spalthoff, S., Nolff, M., Tavassol, F., Essig, H., Stuehmer, C., Bormann, K., Rücker, M., Gellrich, N., 2010. Prefabrication of vascularized bioartificial bone grafts in vivo for segmental mandibular reconstruction: experimental pilot study in sheep and first clinical application. Int. J. Oral Maxillofac. Surg. 39 (4), 379–387.

Liu, F., Ferreira, E., Porter, R., Glatt, V., Schinhan, M., Shen, Z., Randolph, M., Kirker-Head, C., Wehling, C., Vrahas, M., Evans, C., Wells, J., 2015. Rapid and reliable healing of critical size bone defects with genetically modified sheep muscle. Eur. Cells Mater. 30, 118–131.

Liu, F., Porter, R., Wells, J., Glatt, V., Pilapil, C., Evans, C., 2011. Evaluation of BMP-2 gene-activated muscle grafts for cranial defect repair. J. Orthop. Res. 30 (7), 1095–1102.

Malaval, L., Modrowski, D., Gupta, A., Aubin, J., 1994. Cellular expression of bone-related proteins during in vitro osteogenesis in rat bone marrow stromal cell cultures. J. Cell. Physiol. 158 (3), 555–572.

Maruyama, Z., Yoshida, C., Furuichi, T., Amizuka, N., Ito, M., Fukuyama, R., Miyazaki, T., Kitaura, H., Nakamura, K., Fujita, T., Kanatani, N., Moriishi, T., Yamana, K., Liu, W., Kawaguchi, H., Nakamura, K., Komori, T., 2007. Runx2 determines bone maturity and turnover rate in postnatal bone development and is involved in bone loss in estrogen deficiency. Dev. Dyn. 236 (7), 1876–1890.

Merritt, E., Cannon, M., Hammers, D., Le, L., Gokhale, R., Sarathy, A., Song, T., Tierney, M., Suggs, L., Walters, T., Farrar, R., 2010. Repair of Traumatic Skeletal Muscle Injury with Bone-Marrow-Derived Mesenchymal Stem Cells Seeded on Extracellular Matrix. Tissue Eng. Part A 16 (9), 2871–2881.

Miao, C., Zhou, L., Tian, L., Zhang, Y., Zhang, W., Yang, F., Liu, T., Tang, S., Liu, F., 2017. Osteogenic Differentiation Capacity of In Vitro Cultured Human Skeletal Muscle for Expedited Bone Tissue Engineering. Biomed Res. Int. 2017, 1–7.

Oryan, A., Alidadi, S., Moshiri, A., Maffulli, N., 2014. Bone regenerative medicine: classic options, novel strategies, and future directions. J. Orthopaed. Surg. Res. 9 (1), 18.

Patel, Z., Young, S., Tabata, Y., Jansen, J., Wong, M., Mikos, A., 2008. Dual delivery of an angiogenic and an osteogenic growth factor for bone regeneration in a critical size defect model. Bone 43 (5), 931–940.

Pogrel, M., Podlesh, S., Anthony, J., Alexander, J., 1997. A comparison of vascularized and nonvascularized bone grafts for reconstruction of mandibular continuity defects. J. Oral Maxillofac. Surg. 55 (11), 1200–1206.

Porzionato, A., Sfriso, M., Pontini, A., Macchi, V., Petrelli, L., Pavan, P., Natali, A., Bassetto, F., Vindigni, V., De Caro, R., 2015. Decellularized Human Skeletal Muscle as Biologic Scaffold for Reconstructive Surgery. Int. J. Mol. Sci. 16 (12), 14808–14831.

Schliephake, H., 2009. Tissue Engineering in Maxillofacial Surgery. Fundam. Tissue Eng. Regenerat. Med., 827–837

Simonsen, J., Rosada, C., Serakinci, N., Justesen, J., Stenderup, K., Rattan, S., Jensen, T., Kassem, M., 2002. Telomerase expression extends the proliferative life-span and maintains the osteogenic potential of human bone marrow stromal cells. Nat. Biotechnol. 20 (6), 592–596.

Spicer, P., Kretlow, J., Young, S., Jansen, J., Kasper, F., Mikos, A., 2012. Evaluation of bone regeneration using the rat critical size calvarial defect. Nat. Protoc. 7 (10), 1918–1929.

Takagi, K., Urist, M., 1982. The Reaction of the Dura To Bone Morphogenetic Protein (BMP) in Repair of Skull Defects. Ann. Surg. 196 (1), 100–109.

Villalona, G., Udelsman, B., Duncan, D., McGillicuddy, E., Sawh-Martinez, R., Hibino, N., Painter, C., Mirensky, T., Erickson, B., Shinoka, T., Breuer, C., 2010. Cell-Seeding Techniques in Vascular Tissue Engineering. Tissue Eng. Part B: Rev. 16 (3), 341–350.

Zhang, Chan, C., 2010. Isolation and enrichment of rat mesenchymal stem cells (MSCs) and separation of single-colony derived MSCs. Journal of Visualized Experiments. https://doi.org/10.3791/1852.